Original Research Article

Effect of Activated Carbon on Re-Conversion Reaction of Cu/LiCl/C Electrode with $LiPF_6$/Methyl Difluoroacetate Electrolyte

.

ABSTRACT

Transition-metal chlorides are known to suffer from dissolution in organic solvents. However, our previous investigation revealed that in the Li/$CuCl_2$ battery, the dissolution of $CuCl_2$ cathode materials could be suppressed by using $LiPF_6$/methyl difluoroacetate (MFA; CHF_2COOCH_3) electrolyte. And, the Cu/LiCl electrode could both charge and discharge in $LiPF_6$/methyl difluoroacetate (MFA) electrolyte as the re-conversion reaction cathode of Li/$CuCl_2$ battery. However, the capacity is only half the theoretical value of 399 mAh g^{-1}. This is because cuprous is hardly oxidized to cupric during charging due to copper disproportionation reaction.

In this study, activated carbon was added to the Cu/LiCl electrode in order to promote the production of $CuCl_2$, and to improve the capacity. The physical properties of the activated carbon were found to have significant effects: activated carbon with a large specific surface area and micropore volume enabled $CuCl_2$ deposition, and improved the capacity of the Cu/LiCl/C electrode to approximately 300 mAh g^{-1}.

Keywords: Lithium ion battery; Li/$CuCl_2$ battery; MFA; Activated carbon, conversion; re-conversion.

1. INTRODUCTION

Lithium-ion batteries (LIBs) are being widely used in electronic applications (e.g., portable devices), electrical vehicles (EVs), electric energy storage system (EES or ESS), and electrical power control system of photovoltaic and/or wind-turbine power generation. Both existing and new applications demand ever higher performance in LIBs, in terms of energy density, power, volume, safety, price, and environmental impact [1]-[3]. Currently, the electrical energy density of conventional LIBs is approaching the theoretical limit, which is imposed by the intercalation/de-intercalation mechanism of Li^+ ions in the host material. In order to achieve 2–5 times the current energy density needed for future applications, LIBs based on new concepts are required.

Many studies have been conducted on improving the cathode, anode, and electrolyte materials in LIBs [4]-[10].The main limiting factors for the capacity are the phase stability of these materials, and the number of lithium ions exchanged. One new research focus is cathode materials based on conversion reactions. In conventional electrode materials, the Li^+ intercalation/deintercalation processes do not change the material's crystal structure. In contrast, the conversion-type materials undergo complete structural and chemical changes during charge and discharge. Such a process involves a much larger number of electrons,

which enable them to achieve extremely high capacities. Specifically, the conversion reaction related to an irreversible structural change can be expressed by the following equation [7]

$$M_aX_b + nbLi^+ + nbe^- \rightleftarrows bLi_nX + aM \qquad (1)$$

where M is a transition metal (Cu, Fe, Co, Ni, Bi, etc.), X is an anion (O, F, S, N, P, etc.), and b is the formal oxidation state of X (n = 1–3). Redox reactions (1) between the cathode material M_aX_b and Li ions involve the full reduction of the transition metals to their metallic states in the cathode, thereby delivering remarkably higher capacity than intercalation-based LIBs. The Li/$CuCl_2$ battery is attractive in terms of its high voltage (3.07 V vs. Li^+/Li) and high theoretical capacity (399 mAh g^{-1}) due to the two-electron redox reactions of $CuCl_2 + 2Li^+ + 2e^- \rightleftarrows Cu + 2LiCl$. Li/$CuCl_2$ batteries also exhibit lower overvoltage at discharge and charge, compared to other conversion-based LIBs. However, transition-metal chlorides have received little attention for conversion-based LIBs, due to their propensity for dissolution in non-aqueous electrolytes [11],[12].Nevertheless, our recent studies revealed that the electrolyte $LiPF_6$/methyl difluoroacetate (MFA) is effective for suppressing the self-discharge in Li/$CuCl_2$ batteries [13].

Meanwhile, many studies have been conducted on the electrochemical properties of batteries using Li/transition-metal fluorides [14]-[25], sulfides [26]-[40], and oxides [41]-[54]. Most of the published results are concerned with discharge starting from the M_aX_b electrode, while very few focus on charge starting from the M/Li_nX electrode [55],[56]. If the charge-starting re-conversion-based LIBs could be realized by using the M/Li_nX electrode, there would be the new possibilities of Li storage and the adoption of graphite as the anode. During the re-conversion reaction, the Li^+ ions are supplied by Li_nX in the cathode. Therefore, the Li metal anodes can be substituted by graphite anodes, leading to greatly enhanced battery safety. Since the conventional intercalation-type LIB already uses graphite anodes, merely changing the cathode to the M/Li_nX electrode can create the conversion reaction-based cell with much higher energy density. In the Li/$CuCl_2$ batteries, this would mean charge starting from the Cu/LiCl or Cu/LiCl/C electrodes as re-conversion reaction cathodes, instead of discharge starting from the $CuCl_2$/C electrode.

In a previous paper, charge and discharge on the Cu/LiCl electrode were found to be possible in $LiPF_6$/MFA electrolyte even without additional carbon in the electrode. Nevertheless, the resulting low capacity (150 mAh g^{-1}) requires improved $CuCl_2$ formation. In industrial corrosion control, activated carbon is commonly used to remove adsorbed chlorine ions in aqueous solutions in order to protect copper metal. Therefore, we expect that in the Cu/LiCl electrode, the chlorine ion concentration (activity) in the reaction field for $CuCl_2$ formation can be similarly controlled by adding carbon-based adsorbents. In this work, we investigate the influence of different carbon additives on the charge-starting Cu/LiCl/C re-conversion reaction cathodes for LIBs. We also examine the effect of $LiPF_6$/MFA on the formation/deposition of $CuCl_2$, and on improving Cu utilization efficiency and charge/discharge capacities. The mechanisms of the re-conversion reaction in Cu/LiCl/C electrode with $LiPF_6$/MFA are proposed as follows: micropores in the added carbon control the ion concentrations in the electrochemical reaction field, especially that of the chlorine ion, thereby promoting the formation of $CuCl_2$.

2. EXPERIMENTAL DETAILS

Cu/LiCl and Cu/LiCl/C electrodes and $LiPF_6$/MFA electrolyte were prepared under dry conditions (O_2 concentration: < 1 ppm; dew point: < –80 ℃) inside an Ar-filled glove box

(Miwa Mfg. Co. Ltd.). The Cu/LiCl/C cathodes were prepared by mixing Cu powder (Kojundo Chemical Laboratory Co. Ltd, CUE08PB), anhydrous LiCl (Sigma-Aldrich Co. LLC, 429457-25G), a carbon material (glassy carbon (ALS Co., Ltd, S-12), activated carbon A (UES Co., Ltd, UCG-CPT) or B (Asahi Organic Chemicals Industry Co., Ltd, AC-0230)), and polytetrafluoroethylene (PTFE; Du Pont-Mitsui Fluorochemicals Co. Ltd., 6J).

The weight ratio was Cu:LiCl:C:PTFE = 32:48:15:5. The content of the $CuCl_2$/acetylene black (AB) electrode was $CuCl_2$:AB:PTFE=70:25:5, which corresponds to Cu:LiCl:C:PTFE=28:42:25:5 in the Cu/LiCl/C electrode. However, the AB particles have very different size from that of activated carbon. Considering that charge and discharge are possible in the carbonless Cu/LiCl electrode, we decided to use a lower ratio of carbon (15 wt%) in order to isolate the effect of Cl^- adsorption on charge-discharge performance. Additionally, the actual performance was poor with 25 wt% activated carbon.
The Cu/LiCl cathode electrode was prepared by mixing Cu powder, anhydrous LiCl, and PTFE in a weight ratio of Cu:LiCl:PTFE = 40:50:10.

Prior to mixing, LiCl was ground in a mortar to crush the particles to ~10 micron in size. Each carbon material was dried at 200 ℃ under vacuum condition for 24 h. The cathode materials were mixed in a mortar and rolled into a 150 μm-thick sheet. Discs (φ = 5 mm) were punched out of the sheet, and pressed onto a Pt mesh (Sanwakinzoku Co., 100 mesh) at 10 MPa to prepare the Cu/LiCl and Cu/LiCl/C electrodes. Pure lithium foil (thickness: 200 μm, Honjo Metal Co. Ltd.) was used as the counter electrode. MFA (Tokyo Chemical Industry Co. Ltd.) was used as the electrolyte solvent. Its water content was ≤ 50 ppm and the purity was > 99%. The Li salt, $LiPF_6$, was dissolved in MFA at 2.2 mol L^{-1}, as a previous study showed that this concentration produced the lowest self-discharge [13].

A three-electrode electrochemical cell (EC Frontier Co. Ltd.) was used for the charge/discharge measurements. The cell was assembled in Ar-filled glove box, with the cathode, counter electrode, and Li metal wire (φ = 1 mm, Honjo Metal Co. Ltd.) as the reference electrode. The charge and discharge measurements of the cell were performed sequentially in the glove box at room temperature with a potentio/galvanostat (Bio-Logic Science Instruments SAS, VSP-300, SP-200). The highest charge and lowest discharge voltages were 4.0 and 2.5 V, respectively, and the charge/discharge current rate was kept constant at 0.01 C.

The microstructure of the Cu/LiCl/C electrode was characterized by X-ray diffraction (XRD; Bruker Co. D8 ADVANCE). The specific surface area and pore volume of each carbon material were measured by a high-precision gas/vapor adsorption measurement instrument (MicrotracBEL Corp. Belsorp-max), using Brunauer–Emmett–Teller (BET), t-plot, and Barrett-Joyner-Halenda (BJH) methods.

3. RESULTS AND DISCUSSION

3.1 Electrochemical reactions of Li/$CuCl_2$ batteries

The fundamental electrochemical reactions of Li/$CuCl_2$ batteries consist of the following single-electron redox reaction equations (2) and (3), which together can be described by the two-electron reaction in (4)

$$CuCl_2 + Li^+ + e^- \rightleftarrows CuCl + LiCl \text{ (3.41 V vs. } Li^+/Li) \quad (2)$$
$$CuCl + Li^+ + e^- \rightleftarrows Cu + LiCl \text{ (2.74 V vs. } Li^+/Li) \quad (3)$$

$$CuCl_2 + 2Li^+ + 2e^- \rightleftarrows Cu + 2LiCl \ (3.07\ V\ vs.\ Li^+/Li) \quad (4)$$

The formation and deposition of $CuCl_2$ in reaction (2) are difficult, and the plateau at 3.4 V during discharge was scarcely seen in our previous study [13],[57]. This would be caused by the disproportionation reactions with coexisting Cu^{2+}, Cu^+, and Cu^0. Consequently, $CuCl_2$ did not form or deposit on the electrode in the first discharge-charge process, according to X-ray absorption fine structure (XAFS) analysis. Only CuCl and Cu were detected when the cathode electrode was fully charged [57]. In this study, we investigate the possibility of using carbon additives in the cathode material to control the ion concentration in the electrochemical reaction fields.

The adsorptive property of activated carbon could suppress the dissolution of active materials in the LiCl/C electrode. The electrochemical reactions in the pores of activated carbon could also promote the formation and deposition of $CuCl_2$, and improve the Cu utilization efficiency. Consequently, the charge and discharge capacities could be increased.

3.1 Properties of carbon additives

The properties of the two activated carbon materials are shown in Table 1, with those of glassy carbon and acetylene black as references. Both activated carbon A and B have very high specific surface area and total pore volume (measured by BET method). The results of t-plot method indicate that the micropores were well-developed. The specific surface areas measured with BJH-method were used to assess the mesoporosity of the materials, which was quite high for A and B according to Table 1. In both activated carbons, the micropores were more developed than the mesopores, and the total specific surface area was mostly within the material (i.e., in pores) rather than on the surface. The micropores are expected to provide adequate sites for electrochemical reaction, and to suppress the dissolution of active cathode materials.

The properties of acetylene black (DENKA BLACK) are also listed in Table 1. However, its primary particles are very different in size. Therefore, it was excluded from electrochemical experiments in this study. The specific surface area of acetylene black is confirmed to depend on the particle size, and the larger particle size requires a higher content to create a sufficiently large specific surface area. However, the nonporous AB particles contained little internal or external pores according to its adsorption isotherms; therefore it is not suitable as an additive in the Cu/LiCl electrodes.

Table 1. Physical properties of different carbon materials used in the Cu/LiCl/C electrode. Glassy carbon and acetylene black are listed as references

	Acetylene Black	Glassy Carbon	Activated Carbon A	Activated Carbon B
Specific surface area (BET, m^2/g)	55	2	1780	2960
Primary particle size (μm)	0.043	5.0	6.5	2.2
Total pore volume (BET, cm^3/g)	0.18	0	0.86	1.9
Average pore diameter (nm)	13.2	11	1.9	2.5

Total specific surface area (t-plot, m^2/g)	63	3	1700	3710
・Outer	—	—	60	72
・Inner	—	—	1640	3640
Inner pore volume (t-plot, cm^3/g)	—	0	0.75	1.7
Specific surface area (BJH, m^2/g)	59	2.3	241	1460
Total Pore volume (BJH, cm^3/g)	0.3	0	0.24	1.0

3.1 Charge and discharge characteristics of Cu/LiCl/C composite

The charge and discharge profiles of the Cu/LiCl electrode (Cu:LiCl:PTFE = 40:50:10) with 2.2 M $LiPF_6$/MFA is shown in Fig. 1 as a reference. This electrode was verified as a feasible re-conversion reaction cathode with $LiPF_6$/MFA for charge and discharge, without using carbon as conductive additive in the preceding paper. The ratio of Cu:LiCl was chosen to be stoichiometric for synthesizing $CuCl_2$, and the capacity was based on the total weight of Cu and 2LiCl within the electrode. The as-prepared Cu/LiCl electrode had poor conductivity; therefore, the charged voltage was high and the charged capacity low during the first charge–discharge cycle. However, from the second cycle on, this electrode could be charged without the excess voltage shown in the initial cycle. The reason is that the fine copper particles precipitated on the electrode to form an electron transfer path, thereby acting as a conductive material in place of carbon.

However, the capacity of the Cu/LiCl electrode only reached half of its theoretical capacity (399 mAh g^{-1}). The obvious plateau at 2.7 V was attributed to the electrochemical reaction in equation (3), while the mild plateau at about 3.4 V was attributed to equation (2). The plural electrochemical reactions, such as $CuCl \rightarrow Cu^{2+} + Cl^- + e^-$ (3.6 V vs. Li^+/Li), and/or $Cu \rightarrow Cu^+ + e^-$ (3.6 V vs. Li^+/Li) would occur at the same time in the charge process. During discharge, an initial plateau at 3.4 V corresponding to reaction (2) was observed, but it was not extended. The plateau at 2.7 V was observed clearly. These behaviors are assumed to be due to the copper disproportionation reactions.

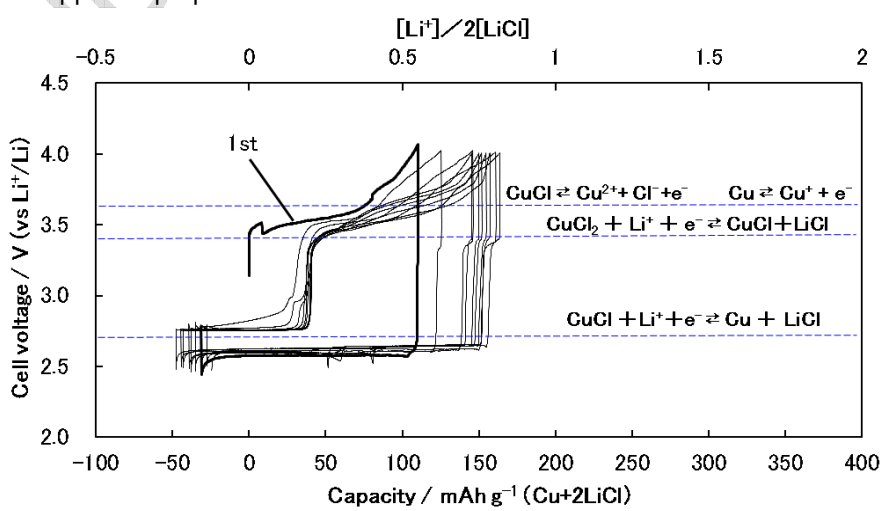

Fig. 1. Charge and discharge profiles of the Cu/LiCl electrode in $LiPF_6$/MFA electrolyte

Fig. 2 shows the charge and discharge profiles of the Cu/LiCl/C electrodes with 2.2 mol L^{-1} $LiPF_6$/MFA, where C = glassy carbon. The overvoltage in the initial charge became lower with glassy carbon. After the second charge process, the clear plateau at 2.7 V was observed first. The mild sloping plateau near 3.4 V became more extended which would be attributed to the simultaneous electrochemical reactions, such as CuCl + LiCl→ $CuCl_2$ + Li^+ + e^- (3.4 V vs. Li^+/Li), CuCl→ Cu^{2+} + Cl^- + e^- (3.6 V vs. Li^+/Li), and/or Cu → Cu^+ + e^- (3.6 V vs. Li^+/Li). The extension of the sloping plateau at 3.4 V suggests that $CuCl_2$ formation and deposition could occur on the Cu/LiCl/C electrode. Accordingly, a plateau at 3.4 V due to Cu reduction (2) was observed during discharge, and the total capacity also increased to nearly 250 mAh g^{-1}.

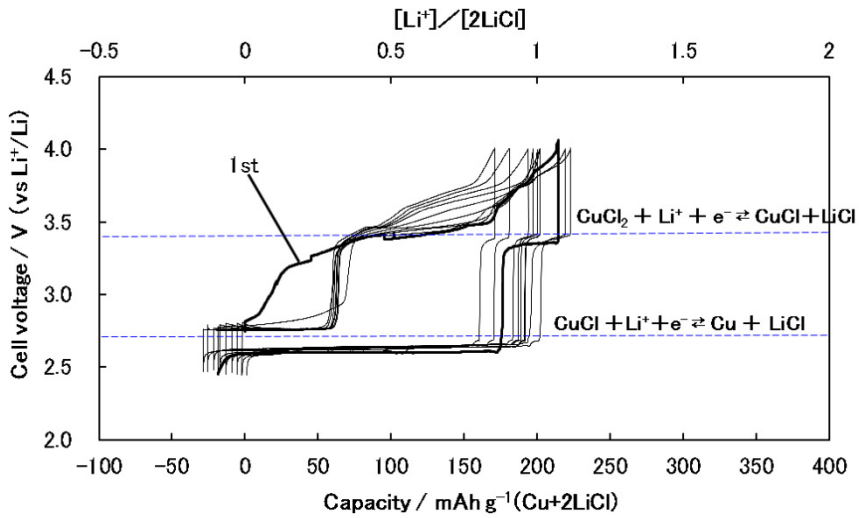

Fig. 2. Charge and discharge profiles of the Cu/LiCl/C electrode, with C = glassy carbon

As shown in Table 1, even though glassy carbon consisted of large particles with very few pores and a smaller specific surface area, its presence effectively increased the charged capacity due to the enhanced formation and deposition of $CuCl_2$ with equation (2). The increased $CuCl_2$ deposition would also enhance the conductivity of the Cu/LiCl/C electrode, as explained earlier. The capacity of ~250 mAh g^{-1} could be further improved by using carbon additives with more suitable properties.

Fig. 3 shows the charge and discharge profiles of the Cu/LiCl/C electrode with C = activated carbon A. The overvoltage in the initial charge process became lower than that in glassy carbon (Fig. 2), and the plateaus at 3.2 V and near 3.4 V appeared clearly in the initial charge process. The plateau at 3.2 V would be attributed to the electrochemical reaction of Cu + Cl^-→CuCl + e^- (3.2 V vs. Li^+/Li). This reaction seems to be caused by LiCl, which is slightly soluble in the Cu/LiCl/C electrode. The second mild slope plateau near 3.4 V would be attributed to reaction (2), as discussed above. The plateau at about 3.6 V would be attributed to the plural electrochemical reactions CuCl→ Cu^{2+} + Cl^- + e^-, and/or Cu → Cu^+ + e^-.

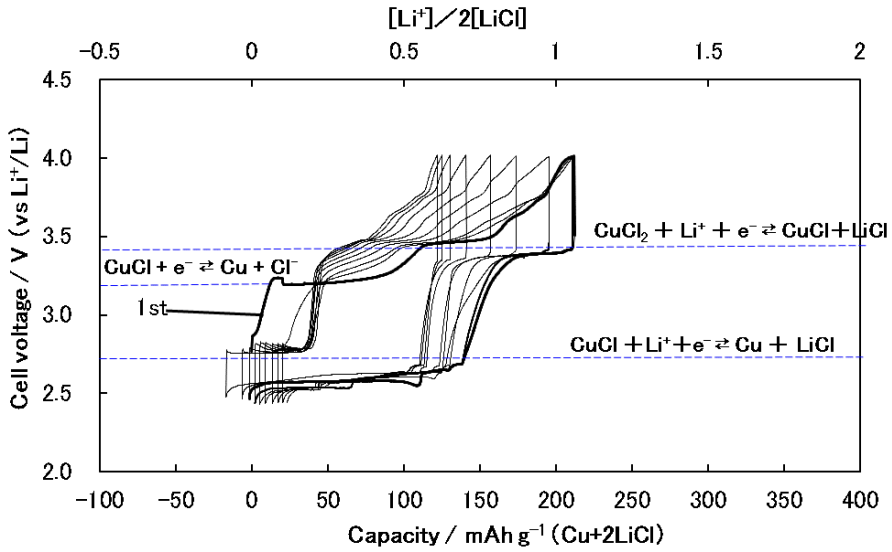

Fig. 3. Charge and discharge profiles of the Cu/LiCl/C electrode, with C = activated carbon A

A comparison of Fig. 2 and Fig. 3 shows that the second mild slope plateau near 3.4 V appeared clearly in the charge process with glassy carbon and activated carbon A. In the discharge process, the plateau at 3.4 V attributed to the Cu reduction reaction (2) became more extended in Fig. 3. The large specific surface area and pore volume (especially that from micropores) of activated carbon A are believed affect the ion concentration (especially that of Cl^-) in an electrochemical reaction field, thereby promoting the formation and deposition of $CuCl_2$ and suppressing the dissolution of active cathode materials. Following repeated charge and discharge, the plateau at 3.2 V gradually shifted to 3.4 V and disappeared, because the corresponding reaction was hindered by the accumulated deposits (e.g. LiF) at the opening of the micropores in the activated carbon.

Fig. 4 shows the charge and discharge profiles of the Cu/LiCl/C electrode using activated carbon B. Compared to activated carbon A (Fig. 3), the overvoltage in the initial charge was lowered, and the plateaus at 3.2 V and ~3.4 V appeared more clearly and extended further compared to activated carbon (Fig. 3). The charge capacity was increased to near 300 mAh g^{-1}.

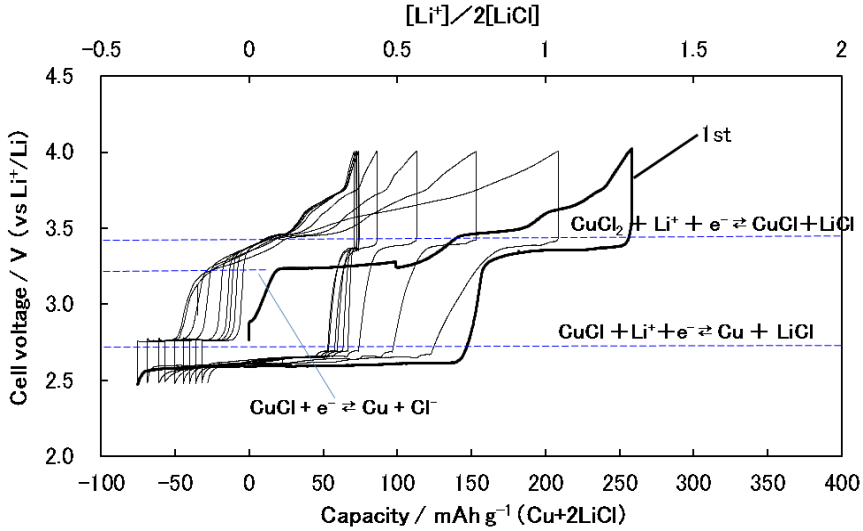

Fig. 4. Charge and discharge profiles of the Cu/LiCl/C electrode, with C = activated carbon B

The main difference between Fig. 3 and Fig. 4 is the length of each plateau, with the longer plateau corresponding to higher capacity. Change of the plateau at 3.4 V especially contributes to the increased total capacity. According to these figures and Table 1, the larger the specific surface area and pore volume, the longer the plateaus at 3.2 and 3.4 V in the initial charge, and also the longer the plateau of 3.4 V due to Cu reduction reaction (2) in the discharge process.

Thus, we confirmed that the specific surface area and pore volume of the carbon additive greatly influence the electrochemical reactions in the charge and discharge processes of the Cu/LiCl/C electrode. This occurs through changing the ion concentration in electrochemical reaction fields, especially within the micropores. While the $LiPF_6$/MFA electrolyte suppressed the dissolution of active materials, the activated carbon was confirmed to promote the formation and deposition of $CuCl_2$ and to further suppress the dissolution of active cathode materials. However, data in Fig. 4 show a gradual decline in these improvements, presumably due to the capture of reactants in the micropores. It is important to address this problem in the future.

Next, we discuss the effect of the microstructure of carbon materials (namely the specific surface area and pore volume) on the formation and deposition of $CuCl_2$. From Fig. 5, the initial discharge capacity corresponding to the Cu reduction reaction (2) (3.4 V) has good linear correlation with the specific surface area of the carbon material. Thus, activated carbon with large specific surface area strongly promotes the formation and deposition of $CuCl_2$. A similar linear relationship is visible in Fig. 6, between the initial discharge capacity and the pore volume of the carbon material in each Cu/LiCl/C electrode. Hence, the pore volume of activated carbon also strongly influences the formation and deposition of $CuCl_2$. A plausible explanation for the above correlations is as follows. The development of micropores increased the specific surface area of the carbon material. The ion concentration in the electrochemical reaction fields can be readily changed within the micropores, thereby enabling the formation of $CuCl_2$ that could not be achieved previously. Other carbon materials rich in micropores, such as carbon nanotubes, are expected to have similar effects.

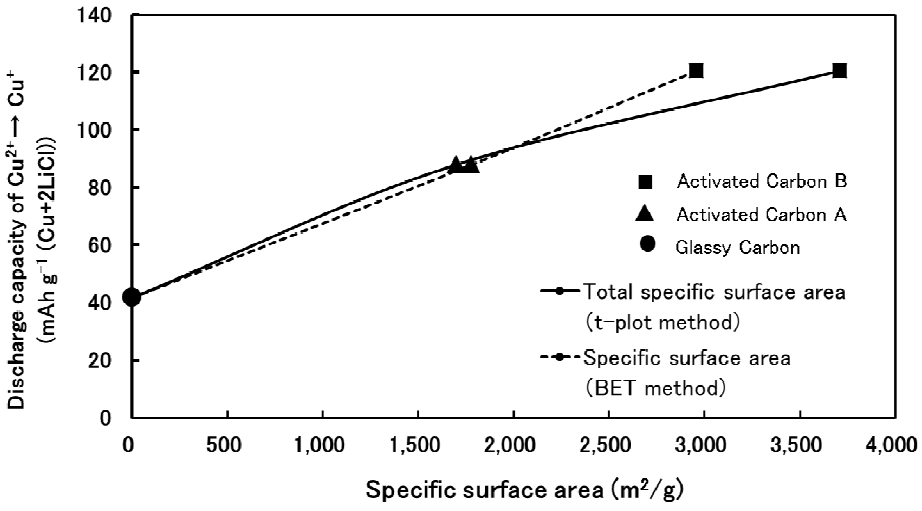

Fig. 5. Relationship between the initial discharge capacity corresponding to Cu reduction reaction (2), and the specific surface area of the carbon additive

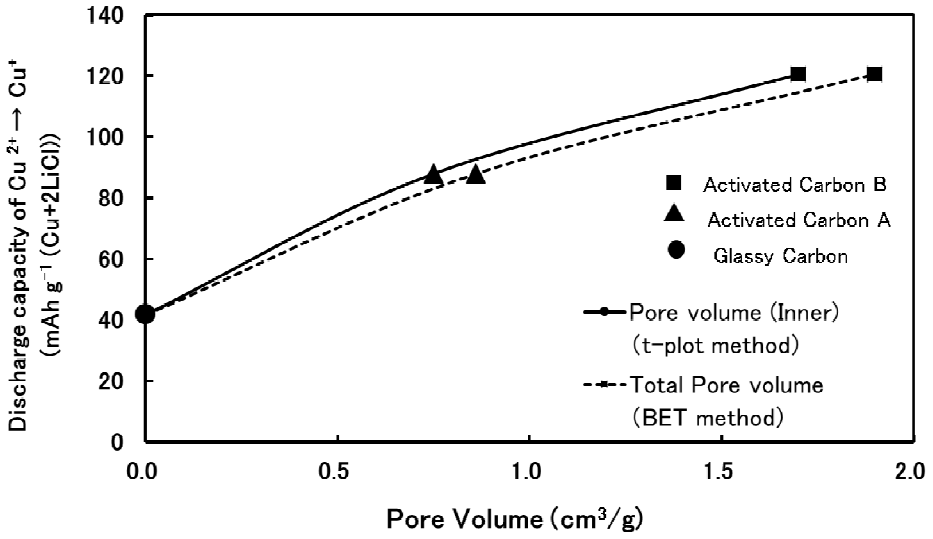

Fig. 6. Relation to initial discharge capacities that correspond to the Cu reduction, equation (2), and pore volumes of activated carbons in each Cu/LiCl/C electrode

To verify that $CuCl_2$ was actually formed and deposited in the Cu/LiCl/C electrode at the full charged condition, the XRD patterns of Cu/LiCl/C electrode after the initial charge are displayed in Fig. 7, together with the typical patterns of $CuCl_2$ and CuCl for reference.

Previous studies of the Cu/LiCl electrode under the fully charged condition only showed signals of CuCl and Cu, not $CuCl_2$ [57]. When activated carbon B was added, $CuCl_2$ signal was confirmed together with that of CuCl. Presumably, the reaction forming $CuCl_2$ would occur in pores, especially the micropores of activated carbon. The pores also helped to suppress the dissolution of active cathode materials, thereby facilitating $CuCl_2$ deposition on the Cu/LiCl/C electrode.

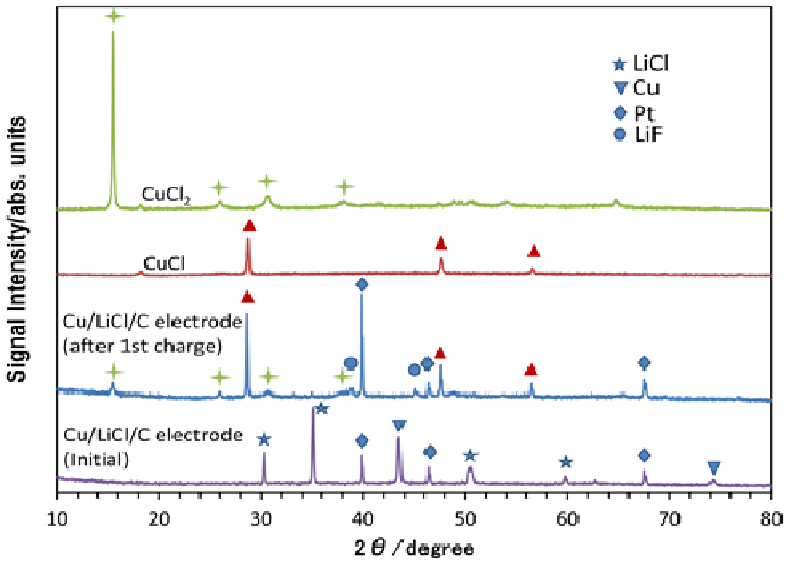

Fig. 7. XRD patterns of the Cu/LiCl/C electrode after the initial charge, $CuCl_2$, and CuCl

4. CONCLUSION

This study used activated carbon in the Cu/LiCl electrode to enhance the $CuCl_2$ formation, and the following results were obtained.

1) Similar to the Cu/LiCl electrode, the Cu/LiCl/C electrode containing activated carbon can also charge-discharge as re-conversion reaction cathodes with $LiPF_6$/MFA electrolyte. The charged capacity was improved from 200 to 300 mAh g^{-1}.

2)The discharge plateau at 3.4 V (vs Li^+/Li) corresponding to $CuCl_2 + Li^+ + e^- \rightarrow CuCl + LiCl$ was observed. The specific surface area and pore volume (especially the micropore volume) of additive carbon are linearly correlated with the capacity in the initial discharge process.

3) XRD analysis confirmed that the Cu/LiCl/C electrode with activated carbon contained $CuCl_2$ after full charge, which is believed to be formed and deposited within the micropores.

4) Other porous carbon materials such as carbon nanotubes are expected to have similar functions as activated carbon.

REFERENCES

1. B. Dunn, H. Kamath and J. M. Tarascon, Science, 334, 928 (2011).
2. V. Etacheri, R. Marom, R. Elazari, G. Salitra and D. Aurbach, Energy Environ. Sci., 4, 3243 (2011).
3. J. M. Tarascon and M. Armand, Nature, 414, 359 (2001).
4. S. Goriparti, E. Miele, F. De Angelis, E. Di Fabrizio, R. P. Zaccaria, and C. Capiglia, J. Power Sources, 257, 421 (2014).
5. Y. N. Zhou, M. Z. Xue, and Z. W. Fu, J. Power Sources, 234, 310 (2013).
6. B. Scrosati, and J. Garche, J. Power Sources, 195, 2419 (2010).
7. J. Cabana, L. Monconduit, D. Larcher, and M. R. Palacín, Adv. Mater., 22, E170 (2010).
8. M. R. Palacín, Chem. Soc. Rev., 38, 2565 (2009).
9. R. Malini, U. Uma, T. Sheela, M. Ganesan, and N. G. Renganathan, Ionics., 15, 301 (2009).
10. P. G. Bruce, B. Scrosati, and J. M. Tarascon, Angew. Chem. Int. Ed., 47, 2930 (2008).
11. J. L. Liu, W. J. Cui, C. X. Wang, and Y. Y Xia, Electrochem. Commun., 13, 269 (2011).
12. T. Li, Z. X. Chen, Y. L. Cao, X. P. Ai, and H. X. Yang, Electrochim. Acta, 68, 202 (2012)
13. S. Dobashi, K. Hashizaki, H. Yakuma, T. Hirai, J. Yamaki, and Z. Ogumi, J. Electrochem. Soc., 162 (14), A2747 (2015).
14. H. Arai, S. Okada, Y. Sakurai, and J. Yamaki, J. Power Sources, 68, 716 (1997).

15. F. Badway, N. Pereira, F. Cosandey, and G. G. Amatucci, J. Electrochem. Soc., 150 (9), A1209 (2003).
16. F. Badway, F. Cosandey, N. Pereira, and G. G. Amatucci, J. Electrochem. Soc., 150 (10), A1318 (2003).
17. H. Li, P. Balaya, and J. Maier, J. Electrochem. Soc., 151 (11), A1878 (2004).
18. Z. W. Fu, C. L. Li, W.Y. Liu, J. Ma, Y. Wang, and Q. Z. Qin, J. Electrochem. Soc., 152 (2), E50 (2005).
19. I. Plitz, F. Badway, J. Al-Sharab, A. DuPasquier, F. Cosandey, and G. G. Amatucci, J. Electrochem. Soc., 152 (2), A307 (2005).
20. Y. Makimura, A. Rougier, L. Laffont, M. Womes, J. C. Jumas, J. B. Leriche, and J. M. Tarascon, Electrochem. Commun., 8, 1769 (2006).
21. F. Badway, A. N. Mansour, N. Pereira, J. F. Al-Sharab, F. Cosandey, I. Plitz, and G. G. Amatucci, Chem. Mater., 19, 4129 (2007).
22. H. Zhang, Y. N. Zhou, Q. Sun, and Z. W. Fu, Solid State Sci., 10, 1166 (2008).
23. T. Li, L. Li, Y. L. Cao, X. P. Ai, and H. X. Yang, J. Phys. Chem. C, 114, 3190 (2010).
24. C. Li, L. Gu, S. Tsukimoto, P. A. van Aken, and J. Maier, Adv. Mater., 22, 3650 (2010).
25. N. Yamakawa, M. Jiang, and C. P. Grey, Chem. Mater., 21, 3162 (2009).
26. F. Bonino, M. Lazzari, B. Rivolta, and B. Scrosati, J. Electrochem. Soc., 131 (7), 1498 (1984).
27. J. S. Chung and H. J. Sohn, J. Power Sources, 108, 226 (2002).
28. S. C. Han, H. S. Kim, M. S. Song, J. H. Kim, H. J. Ahn, J. Y. Lee, and J. Y. Lee, J. Alloys Compd., 351, 273 (2003).
29. A. Hayashi, T. Ohtomo, F. Mizuno, K. Tadanaga, and M. Tatsumisago, Electrochim. Acta, 50, 893 (2004).
30. J. M. Yan, H. Z. Huanga, J. Zhanga, Z. J. Liub, and Y. Yang, J. Power Sources, 146, 264 (2005).
31. A. Debart, L. Dupont, R. Patrice, and J. M. Tarascon, Solid State Sci., 8, 640 (2006)
32. X. J. Zhu, Z. Wen, Z. H. Gu, and S. H. Huang, J. Electrochem. Soc., 153 (3), A504 (2006)
33. Q. Wang, R. Gao, and J. H. Li, Appl. Phys. Lett., 90 (14), 143107 (2007)
34. T. Matsumura, K. Nakano, R. Kanno, A. Hirano, N. Imanishi, and Y. Takeda, J. Power Sources, 174 , 632 (2007)
35. Q. Wang and J. H. Li, J. Phys. Chem. C, 111, 1675 (2007)
36. J. Z. Wang, S. L. Chou, S. Y. Chew, J. Z. Sun, M. Forsyth, D. R. MacFarlane, and H. K. Liu, Solid State Ionics, 179 , 2379 (2008)
37. J. L. Gomez-Camer, F. Martin, J. Morales, and L. Sanchez, J. Electrochem. Soc., 155 (3), A189 (2008)
38. T. Takeuchi, H. Sakaebe, H. Kageyama, T. Sakai, and K. Tatsumi, J. Electrochem. Soc., 155 (9), A679 (2008)
39. H. Li, W. J. Li, L. Ma, W. X. Chen, and J. M. Wang, J. Alloys Compd., 471, 442 (2009).
40. R. D. Apostolova, E. M. Shembel, I. Talyosef, J. Grinblat, B. Markovsky, and D. Aurbach, Russ. J. Electrochem., 45 (3), 311 (2009).
41. P. Poizot, S. Laruelle, S. Grugeon, L. Dupont, and J. M. Tarascon, Nature, 407 (28), 496 (2000).
42. S. Grugeon, S. Laruelle, R. Herrera-Urbina, L. Dupont, P. Poizot, and J. M. Tarascon, J. Electrochem. Soc., 148 (4), A285 (2001).
43. D. Larchera, G. Sudanta, J. B. Lerichea, Y. Chabreb, and J. M. Tarascon, J. Electrochem. Soc., 149 (3), A234 (2002).
44. M. Dolle, P. Poizot, L. Dupont, and J. M Tarascon, Electrochem. Solid-State Lett., 5 (1), A18 (2002).
45. S. Laruelle, S. Grugeon, P. Poizot, M. Dolle, L. Dupont, and J. M. Tarascon, J. Electrochem. Soc., 149 (5), A627 (2002).

46. P. Poizot, S. Laruelle, S. Grugeon, and J. M. Tarascon, J. Electrochem. Soc., 149 (9), A1212 (2002).
47. Z. Yuan, F. Huang, C. Feng, J. Sun, Y. Zhou, Mater. Chem. Phys., 79 (1), 1 (2003).
48. P. Balaya, H. Li, L. Kienle, and J. Maier, Adv. Funct. Mater., 13 (8), 621 (2003).
49. J. Hu, H. Li, and X. Huang, Electrochem. and Solid-State Lett., 8 (1), A66 (2005).
50. W. Y. Li, L. N. Xu, and J. Chen, Adv. Funct. Mater., 15, 851 (2005).
51. F. Jiao, J. Bao, and P. G. Bruce, Electrochem. and Solid-State Lett., 10 (12), A264 (2007).
52. J. Kim, M. K. Chung, B. H. Ka, J. H. Ku, S. Park, J. Ryu, and S. M. Oh, J. Electrochem. Soc., 157 (4), A412 (2010).
53. D. Wadewitz, W. Gruner, M. Herklotz, M. Klose, L. Giebeler, A. Voß, J. Thomas, T. Gemming, J. Eckert, and H. Ehrenberg, J. Electrochem. Soc., 160 (8), A1333 (2013).
54. R. Adam, D. Wadewitz, W. Gruner, V. Klemm, H. Ehrenberg, and D. Rafaja, J. Electrochem. Soc., 160 (9), A1594 (2013)
55. Y. Zhou, W. Liu, M. Xue, L. Yu, C. Wu, X. Wu, and Z. Fu, Electrochem. and Solid-State Lett., 9 (3), A147 (2006).
56. R. Prakash, C. Wall, A. K. Mishra, C. Kubel, M. Ghafari, H. Hahn, and M. Fichtner, J. Power Sources, 196, 5936 (2011).
57. S. Dobashi, K. Nakanishi, H. Tanida, K. Hashizaki, Y. Uchimoto, T. Hirai, J. Yamaki, and Z. Ogumi, J. Electrochem. Soc., 163 (5), A727 (2016).